Molecular Pharmacology Fast Forward. Published on January 23, 2019 as DOI: 10.1124/mol.118.114207
This article has not been copyedited and formatted. The final version may differ from this version.

MOL # 114207

MiR-144 Inhibits Tumor Growth and Metastasis in Osteosarcoma via Dual-suppressing RhoA/ROCK1 Signaling Pathway

Jin Long Liu[1], Jing Li[2], Jia Jia Xu[1], Fei Xiao[1], Peng Lei Cui[1], Zhi Guang Qiao[3], Xiao Ling Zhang[1#]

[1] Department of Orthopedic Surgery, Xin Hua Hospital Affilliated to Shanghai Jiao Tong University School of Medicine (SJTUSM) Shanghai, China., 200092.

[2] The Key Laboratory of Stem Cell Biology, Institute of Health Sciences, Shanghai Institutes for Biological Sciences, Chinese Academy of Sciences & Shanghai Jiao Tong University School of Medicine, China, 200025.

[3] Shanghai Key Laboratory of Orthopedic Implant, Department of Orthopaedic Surgery, Shanghai Ninth People's Hospital, Shanghai Jiao Tong University School of Medicine, China, 200011.

Molecular Pharmacology Fast Forward. Published on January 23, 2019 as DOI: 10.1124/mol.118.114207
This article has not been copyedited and formatted. The final version may differ from this version.

MOL # 114207

Running title: MiR-144 Inhibits Tumor Growth and Metastasis in Osteosarcoma

Correspondence to: xlzhang@shsmu.edu.cn, Department of Orthopedic Surgery, Xin Hua Hospital Affiliated to Shanghai Jiao Tong University School of Medicine (SJTUSM) Shanghai, China.

The number of text pages: 36 pages

The number of figures: 7 figures

The number of references: 42 references

The number of words in the Abstract: 171 words

The number of words in the Introduction: 506 words

The number of words in the Discussion: 759 words

Abbreviations

OS, osteosarcoma; RhoA, Ras homolog family member A; ROCK1, Rho-associated, coiled-coil containing protein kinase 1; 3'-UTR, 3'-untranslated region; miRNAs, microRNAs; mRNAs, messenger RNAs;

Molecular Pharmacology Fast Forward. Published on January 23, 2019 as DOI: 10.1124/mol.118.114207
This article has not been copyedited and formatted. The final version may differ from this version.

Abstract

Several miRNAs have been found expressed differentially in osteosarcoma (OS), thus they may function in the onset and progression of osteosarcoma. In this study, we found that miR-144 significantly suppresses osteosarcoma cell proliferation, migration and invasion ability *in vitro*, and inhibited tumor growth and metastasis *in vivo*. Mechanically, we demonstrated that Ras homolog family member A (RhoA) and its pivotal downstream effector Rho-associated, coiled-coil containing protein kinase 1 (ROCK1) were both identified as direct targets of miR-144. Moreover, the negative co-relation between downregulated miR-144 and upregulated ROCK1/RhoA was verified both in the osteosarcoma cell lines and clinical patients' specimens. Functionally, RhoA with or without ROCK1 co-overexpression resulted a rescue phenotype on the miR-144 inhibited cell growth, migration and invasion abilities, while individual overexpression of ROCK1 had no statistical significance compared with control in miR-144 transfected SAOS2 and U2-OS cells. Taken together, this study demonstrates that miR-144 inhibited tumor growth and metastasis in osteosarcoma via dual-suppressing of RhoA and ROCK1, which could be a new therapeutic approach for the treatment of osteosarcoma.

Molecular Pharmacology Fast Forward. Published on January 23, 2019 as DOI: 10.1124/mol.118.114207
This article has not been copyedited and formatted. The final version may differ from this version.

Introduction

Osteosarcoma (OS) is the most prevalent bone tumor in children and young adults[Bielack, 2008 #1]. Most tumors arise from the metaphysis of the long bones and easily metastasize to the lungs[Harting, 2006 #2;Harting, 2006 #2]. Current therapeutic strategies of osteosarcoma are routinely surgical resection and chemotherapy[Link, 1986 #3], which are limited to the patients suffering from metastatic recurrence. Survival of osteosarcoma patients remains poor, and the 5-year survival rate for patients who have metastasis is about 15 % to 30 %[Mirabello, 2009 #4]. Therefore, to investigate molecular mechanisms that contribute to osteosarcoma progression is very important and may shed light on targeted therapeutic approach to improve the survival of patients with this disease.

MicroRNAs (miRNAs) are small non-coding single-stranded RNAs, which repress gene expression post-transcriptionally by binding to the 3'-untranslated region (3'-UTR) of their target messenger RNAs (mRNAs)[Bartel, 2004 #5;Bartel, 2004 #5]. MiRNAs play critical roles in physiological processes such as cell growth, development and differentiation[Alvarez-Garcia, 2005 #6;Alvarez-Garcia, 2005 #6]. Also, aberrant expression of specific miRNAs leads to the onset and/or deterioration of many diseases, such as cancer[Croce, 2009 #7;Croce, 2009 #7], heart disease[Divakaran, 2008 #8;Divakaran, 2008 #8] and arthritis[Tili, 2008 #9;Tili, 2008 #9]. Recently, several miRNAs have been identified exerting anti-cancer effects by influencing cell proliferation, apoptosis and migration, acting as oncogenes or tumor suppressors[Lu, 2005 #10;Hurst, 2009 #11]. For example, miR-181a has been reported to be up-regulated in osteosarcoma, and correlates with cancer development[Jianwei, 2013 #12]. Rho-associated, coiled-coil containing protein kinase (ROCK) is a key downstream effector of the small GTPase RhoA. Two ROCK isoforms ROCK1 and ROCK2 have been identified in mammalian cells and share 65 % identity in their amino-acid sequences[Nakagawa, 1996 #15]. ROCK1 has a ubiquitous distribution while ROCK2 is mainly expressed in the brain and muscle tissue[Hahmann, 2010 #16]. When activated by Rho-GTP, ROCK phosphorylates several substrates, such as myosin light chain 2 (MLC2)[Leung, 1996 #17], LIM kinase 1 (LIMK1)[Ohashi, 2000 #18] and

Molecular Pharmacology Fast Forward. Published on January 23, 2019 as DOI: 10.1124/mol.118.114207
This article has not been copyedited and formatted. The final version may differ from this version.

LIM kinase 2 (LIMK2) [, !!! INVALID CITATION !!! 13 #19], which leads to the phosphorylation of cofilin[Maekawa, 1999 #20]. RhoA/ROCK pathway mediates a number of cellular functions, including cytoskeleton reorganization, cell mobility, proliferation and survival. Elevated ROCK1 expression has been detected in a spectrum of malignancies, such as breast[Cimino, 2013 #21], prostate[Lin, 2008 #22] and gastric cancer[Zheng, 2011 #23], and this deregulation usually correlates with poor prognosis. Previous studies have shown that ROCK1 is strongly up-regulated in osteosarcoma clinical specimens[Liu, 2011 #24] and may be a therapeutic target of this disease. We wondered whether the deregulation of ROCK1 was associated with miRNA regulation. In this study, we identified miR-144 as a negative regulator of ROCK1 and RhoA by *in silico* miRNA target prediction algorithms. We demonstrated that miR-144 was downregulated in osteosarcoma clinical specimens and cancer cell lines. We revealed for the first time that miR-144 repressed tumorigenesis and metastasis through dual-suppression of RhoA/ROCK1 pathway. Our results indicated that miR-144 played a critical tumor-suppressive role in the process of osteosarcoma progression and could be a potential candidate for the treatment of osteosarcoma.

Molecular Pharmacology Fast Forward. Published on January 23, 2019 as DOI: 10.1124/mol.118.114207
This article has not been copyedited and formatted. The final version may differ from this version.

Materials and Methods

Tissue Specimens

Tissue samples from fifty-one osteosarcoma patients were obtained from Shanghai Ninth People's Hospital. The details of the cases were presented in Table 1. As a control, normal human bone fragments that were isolated from healthy donors who had undergone total knee arthroplasty were obtained from Shanghai Ninth People's Hospital. Informed consent was obtained from all patients prior to conducting the study. The tissues were fixed with 4 % paraformaldehyde for histopathologic diagnosis and immunohistochemical staining.

Cell Culture

All cell lines were obtained from the American Type Culture Collection (ATCC, Manassas, VA). Human osteoblastic cell line hFOB 1.19 was maintained at 33.5 °C in DMEM/F-12 medium (GIBCO) supplemented with 10 % fetal bovine serum (FBS, GIBCO). Human osteosarcoma cell lines SaOS2, U2OS and MG63 were cultured in minimum essential medium alpha (α-MEM, GIBCO) supplemented with 10 % fetal bovine serum (FBS, GIBCO) at 37 °C in humidified atmosphere containing 5 % CO_2.

Cell viability assay

Cell growth was monitored by CCK8 assay as the manufacturer's instructions. Briefly, cells at 5×10^3 per well were incubated in 96-well plates for 0, 24, 48 or 72hours and CCK-8 (Dojindo, Japan) was added into the well. At 4 hours after CCK-8 incubation, cell viability was measured by reading optical density value at a wavelength of 450 nm.

Wound Healing Assay

Cells were seeded into a 6-well culture plate. A scratch wound was created in the center of the cell culture plate with a sterile pipette tip when the cells reached 90 % confluence. Cells were washed by PBS twice to remove the debris. The medium was replaced with α-MEM supplemented with 1 % FBS. Three randomly selected fields along the scraped line were photographed under an inverted microscope. The distance from one side of the scratch to the other was measured using Image Pro-Plus 6.0 software (Media Cybernetics, USA).

Molecular Pharmacology Fast Forward. Published on January 23, 2019 as DOI: 10.1124/mol.118.114207
This article has not been copyedited and formatted. The final version may differ from this version.

Invasion Assay

For the migration assays, 5×10^4 cells were seeded into the upper chamber of the Millicell Hanging Cell Culture inserts (8 μm pore size; Millipore, Billerica, MA, USA). For the invasion assays, 1×10^5 cells were seeded into the upper chamber of the insert coated with Matrigel (BD Bioscience). Chambers were placed in wells with α-MEM containing 10 % FBS. After 24 h of incubation at 37 °C, the non-invading cells were removed by wiping with a cotton swab. Cells that had migrated or invaded through the filter membrane were fixed and stained with Mayer's hematoxylin (Sigma, St. Louis, MO, USA). The number of invading cells on membrane was counted in five microscopic fields (× 400). Experiments were repeated three times in triplicate.

Flow Cytometry

Cells were harvested, washed with cold PBS, and fixed with 75 % cold ethanol at 4 °C overnight. After fixation, cells were collected and incubated with 100 μg/ ml RNase A (Sigma, St. Louis, MO, USA) at 37 °C for 30 min, followed by incubation with 25 μg/ ml propidium iodide (Sigma, St. Louis, MO, USA) at room temperature in the dark. Cell cycle distribution was analyzed by a FACS flow cytometer (Becton Dickinson, Franklin Lakes, NJ, USA).

Biotin-coupled miRNA capture

Approximately 106 cells were transfected with 50 μM of biotinylated miR-144 mimic or ROCK1/RhoA 3'UTR binding site mutant miR-144 mimic (GenePharma, Shanghai, China) at 50% confluence for lysis. At 24 h after transfection, the cells were harvested and washed in PBS, lysed in lysis buffer. A total of 50 μl washed streptavidin magnetic beads were blocked for 2 h and then added to each reaction tube to pull down the biotin-coupled RNA complex. All the tubes were incubated for 4 h on the rotator at a low speed (10 rpm). The beads were washed with lysis buffer for five times and Trizol LS (Life Technology, USA) was used to recover RNAs specifically interacting with miRNA. The abundance of ROCK1 and RhoA 3'UTR in bound fractions was evaluated by qRT-PCR analysis.

Dual-luciferase reporter assays

The ROCK1 and RhoA 3'UTR binding sites of miR-144 were predicted by TargetScan

(http://www.targetscan.org/vert_71/). The different fragment sequences were synthesized and then inserted into the pGL3-basic vector (Promega) by Hanbio (Shanghai, China). All plasmids for transfection were verified by sequencing and prepared using the QIAGEN plasmid purification kit (QIAGEN, Hilden, Germany). HEK293T cells were transiently transfected using Lipofectamine 3000 (Invitrogen, Carlsbad, CA, USA) according to the manufacturer's instructions. Twenty-four hours after transfection, cells were lysed, and Firefly and Renilla luciferase activities were measured using the Dual-Luciferase Reporter Assay System (Promega, Madison, WI, USA) according to the manufacturer's protocol. Each experiment was repeated at least three times.

Lentivirus Production and Infection

The luciferase gene was cut from pGL3-Basic plasmid (Promega, Madison, WI, USA) with NheI and XbaI. Plenti-neo (Invitrogen, Carlsbad, CA, USA) was digested with SpeI and dephosphorylated using calf intestinal phosphatase (CIP). Then the luciferase gene was subcloned into the SpeI site of the plenti-neo thus resulting in the recombinant expression vector plenti-neo-luc. Purified plenti-neo-luc and the packaging mixture were cotransfected into 293FT cells using Lipofectamin 2000 to generate lentivirus, and then the concentrated virus was transduced to SAOS2 cells with 8 μg/ml of polybrene (Sigma, St. Louis, MO, USA). The corresponding cell line stably expressing luciferase was named SAOS2-luc.

Western Blotting Analysis

Whole-cell lysates were prepared with ice-cold lysis buffer (50 mM Tris-HCl, pH 7.4, 150 mM NaCl, 1 % NP-40, and 0.1 % sodium dodecyl sulfate) supplemented with protease inhibitors (Complete Tablet; Roche, Mannheim, Germany). Protein concentration was determined using a Pierce® BCA Protein Assay Kit (Thermo Fisher Scientific, Houston, TX, USA). Proteins were size-fractionated by SDS-PAGE and transferred to a PVDF membrane (Hybond-P; Amersham Biosciences, Amersham, UK). Membranes were incubated overnight at 4 °C with the primary antibodies. Antibodies against ROCK1, RhoA and GAPDH (I-19) were from Santa Cruz Biotechnology (Santa Cruz, CA, USA). After washing with Tris-buffered saline containing 0.1 % Tween

(TBST), membranes were incubated with horseradish peroxidase-conjugated secondary antibodies for 1 hour at room temperature.

RNA Extraction and Quantitative Real-time PCR

Total RNA, including miRNA, was extracted using the miRNeasy Mini Kit (QIAGEN) according to the manufacturer's instructions. Then 1 μg total RNA was reverse-transcribed with a specific stem-loop primer for miRNA. After RT reaction, real-time PCR was performed by an ABI 7900HT system using SYBR Premix ExTaq™ (Takara, Madison,. WI, USA). Small nuclear RNA U6 was used as an internal control for miRNA. Primer sequences used for real-time PCR are presented in Table 2.

Generation of Osteosarcoma Model

Animal handling and experimental procedures were performed following the ethical guidelines of the Shanghai Jiao Tong University School of Medicine. 4- to 6-week-old male nu/nu athymic mice were anesthetized with tribromoethanol. Human osteosarcoma SAOS2-luc cells were injected into the tibia (1×10^7 cells in 50 μL PBS) of athymic mice to induce a tumor[Tu, 2012 #25]. Tumor growth was monitored by measuring 2 perpendicular diameters with digital calipers. Tumor volume was calculated using the formula $V = (L \times W^2)/2$ where L and W represent the largest and the smallest diameter, respectively.

In Vivo Treatment and Bioluminescence Imaging

In vivo jetPEI (Polyplus-Transfection, France) was used as a transfection reagent. JetPEI/miR-144 or jetPEI/negative control complexes with a ratio of 1:7 were prepared in a solution of 10 % w/v glucose. One week after injection of the tumor cells, mice were randomly separated into 2 groups (n = 10 mice per group) and treated by way of multi-point intratumoral injection twice a week, according to the manufacturer's instructions. Tumor growth was monitored over time using an In Vivo Imaging System (IVIS, Xenogen, Alameda, CA). Mice were anesthetized and injected intraperitoneally with D-luciferin. Imaging was performed with an exposure time of 1 min. Upon termination of the experiment, mice were sacrificed. Tumors, lungs and livers were immediately fixed in 4 % paraformaldhyde for paraffin embedding. Sections of 5 μm were stained with Hematoxylin and Eosin and immunohistochemistry. Lungs were

Molecular Pharmacology Fast Forward. Published on January 23, 2019 as DOI: 10.1124/mol.118.114207
This article has not been copyedited and formatted. The final version may differ from this version.

examined microscopically for the presence of OS foci. Also, tumors were spap-frozen for RNA preparation.

Histology and Immunohistochemistry

Osteosarcomas from patients as well as the model animals were fixed overnight with 4 % paraformaldhyde in PBS, decalcified with 12.5 % EDTA, and then embedded in paraffin. Tissue sections (5 μm) were deparaffinized in xylene, serially rehydrated in ethanol, and stained with hematoxylin and eosin. For immunohistochemistry, sections in 10 mM sodium citrate buffer (pH 6.0) were heated in a microwave oven and kept at 95 °C for 10 minutes. Slides were cooled for 30 minutes at room temperature after antigen unmasking. Endogenous peroxidase activity was blocked with 3 % hydrogen peroxide, followed by rinsing several times in PBS. After blocking nonspecific protein binding with 5 % BSA in PBS for 30 minutes at room temperature, sections were incubated overnight at 4 °C with primary antibody against ROCK1 (Santa Cruz) and RhoA (Santa Cruz). The slides were rinsed in PBS and then incubated with secondary antibody (EnVision detection kit, Peroxidase/DAB, Rabbit/mouse; Dako Cytomation, Carpinteria, CA, USA) according to the manufacturer's protocol. After washing, the slides were stained with 3,3'-diaminobenzidine tetrahydrochloride (EnVision detection kit, Peroxidase/DAB, Rabbit/mouse; Dako Cytomation). Sections were counterstained with Mayer's hematoxylin (Sigma, St. Louis, MO, USA). Staining with normal IgG and staining without primary antibody were also performed as negative controls.

Cell Staining and Injections

SAOS2 osteosarcoma cells cultured at 80% density were trypsinized and centrifuged at 1000 rpm for 5 minutes. The supernatant was discarded and resuspended in serum-free α-MEM medium (GIBCO) to 1×10^6 cells / ml, then add 5ul of live cell fluorescence labeling reagent CM-Dil (4ng/ul final concentration) and resuspend. Cells stained with CM-Dil were ncubated at 37 °C for 20 minutes, and centrifuged at 1500 rpm for 5 minutes at 37 °C. Discard the supernatant and resuspend in 100 ul,37 °C PBS for 4-5 times, prepared for injecting into the embryos. The 2dpf zebrafish embryos were anesthetized with anesthetic tricaine, cells labelled with CM-Dil were injected into the yolk sac of 2 days old zebrafish and the cell density was about 2×10^5cells/ul.

Molecular Pharmacology Fast Forward. Published on January 23, 2019 as DOI: 10.1124/mol.118.114207
This article has not been copyedited and formatted. The final version may differ from this version.

Immediately after injection, a fluorescence microscope (Olympus FV1000) was observed and photographed. Remove the uninjected cells and the dead zebrafish embryos. After injection, embryos were incubated at 31°C for 1h then at 35°C,observe and shoot every 24 hours.

Statistical Analysis

Results were expressed as mean ± standard deviation. The P-values in Table 1 were obtained from Pearson chi-square test or Fisher's exact test. The Kaplan-Meier analysis was used to estimate the overall survival, and the log-rank test was used to evaluate the differences between survival curves. The statistical significance of differences between the two groups was calculated by using Student's t test. The other statistical analyses performed were Dunnett's or Tukey-Kramer's tests, as post-hoc tests following the analysis of variance (ANOVA). The details are indicated in Figure legends. $P < 0.05$ was considered statistically significant.

Molecular Pharmacology Fast Forward. Published on January 23, 2019 as DOI: 10.1124/mol.118.114207
This article has not been copyedited and formatted. The final version may differ from this version.

Results

MiR-144 functions as a tumor suppressor in osteosarcoma cells

To evaluate the role of miR-144 in osteosarcoma, we firstly transfected miR-144 mimics or miR-NC into osteosarcoma cells SAOS2 and U2-OS. Transfection of miR-144 mimics significantly suppressed the cell proliferation after 72- and 96-hours' culture, which was determined by CCK8 assay (Figure 1A). To further explore miR-144 role in osteosarcoma cell proliferation, cell cycle distribution was investigated by flow cytometry. miR-144 mimics transfected cells accumulated at the G0/G1 phase of cell cycle (Figure 1B). Soft agar assays showed that miR-144 significantly suppressed the anchorage-independent growth in SAOS2 and U2-OS cells (Figure 1C). Furthermore, we wondered whether miR-144 would cause motility alteration. The results of invasion assays and wound healing assays showed that miR-144 dramatically compromised the invasion and migration abilities of SAOS2 and U2-OS cells (Figure 1D and 1E). Collectively, these results demonstrated that miR-144 functioned as a tumor suppressor in osteosarcoma cells, markedly inhibiting cell growth, migration and invasion abilities.

ROCK1 and RhoA are direct targets of miR-144

Since miR-144 has shown to serve multiple biological functions, especially playing an important role in osteosarcoma cancer etiology, we wondered whether there were certain genes were directly regulated by miR-144 in osteosarcoma. With the help of miRNA target prediction databases TargetScan [Lewis, 2005 #26] (http://www.targetscan.org) and miRanda [Betel, 2008 #27] (http://www.microrna.org), miR-144 was predicted to bind to RhoA and its pivotal downstream effector ROCK1 mRNA, and further analysis was performed. To determine whether miR-144 regulated RhoA and ROCK1 expression, protein levels of RhoA and ROCK1 were examined in control and miR-144 mimics transfected SAOS2 and U2-OS cells. Results demonstrated that RhoA and ROCK1 protein were significantly decreased in miR-144 mimic transfected SAOS2 and U2-OS cells (Figure 2A). Pulldown assay also revealed a more enrichment of ROCK1 and RhoA 3'UTR in the miR-144-captured fraction

Molecular Pharmacology Fast Forward. Published on January 23, 2019 as DOI: 10.1124/mol.118.114207
This article has not been copyedited and formatted. The final version may differ from this version.

compared with the introduction of miR-144 mutation that disrupted the binding site of miR-144 for ROCK1/RhoA 3'UTR (Figure 2B). Moreover, we performed anti-AGO2 RNA immunoprecipitation and examined the miR-144, RhoA and ROCK1 mRNA expression. Results showed that miR-144 was enriched in AGO2-containing complexes, and miR-144 bound to RhoA and ROCK1 mRNA (Figure 2C). To further validate the computational finding that miR-144 negatively regulated RhoA and ROCK1, RhoA and ROCK1 3'-UTR containing the wildtype or mutant miR-144 binding site were cloned into the psiCHECHK^{TM}-2 plasmid (Figure 2D, left). miR-144 mimics significantly repressed the luciferase reporter activity of the wildtype 3'-UTR, while the luciferase reporter activity of the mutant 3'-UTR was not influenced by miR-144 (Figure 2D, right). These results demonstrated that RhoA and ROCK1 are direct targets of miR-144.

MiR-144 inhibits osteosarcoma cells proliferation through dual-inhibition of RhoA 1 and ROCK

Having established the tumor-suppressive role of miR-144 and verified its direct targets RhoA and ROCK1, we further aimed to find out how miR-144 inhibited osteosarcoma tumorigenesis via RhoA/ROCK1 pathway. We transfected ROCK1 and RhoA respectively or co-transfected ROCK1 and RhoA in miR-144 transfected SAOS2 and U2-OS cells using adenovirus infection (Figure 3A). Results suggested that cell growth, migration and invasion abilities equally significantly increased after individual RhoA overexpression and RhoA and ROCK1 co-overexpression in miR-144 transfected SAOS2 and U2-OS cells, while individual overexpression of ROCK1 had no statistical significance compared with control in miR-144 transfected SAOS2 and U2-OS cells (Figure 3B-3E). These results suggested that miR-144 exerted antitumor effects through dual-inhibition of RhoA/ROCK1 pathway. Only ROCK1 rescuing is failed to diminish the antitumor effects of miR-144 in osteosarcoma cells.

MiR-144 inhibits tumorigenesis and metastasis *in vivo*

In order to further confirm the tumor-suppressive role of miR-144 in vivo, we then validated our hypothesis in mice and zebrafish models. Tumorigenic human

osteosarcoma cells SAOS2, stably expressing Firely luciferase, were injected into the tibia of nude mice. Upon establishing the tumor xenografts, mice were intratumorally injected with either miR-144 or NC oligo nucleotides complexed twice a week, and the tumor growth was monitored by bioluminescence imaging. Overexpression of miR-144 dramatically reduced tumor volume of xenografts in nude mice (Figure 4A, 4B). Median survival was shortened by about 2.6 weeks in NC group compared with the miR-144 treated mice as assessed by Kaplan-Meier curves (Figure 4C). In situ hybridization (ISH) and immunohistochemical analysis of tumor sections clearly demonstrated the reduced expression of ROCK1/RhoA in the miR-144 elevated mice (Figure 4D). In addition, human osteosarcoma cells SAOS2 stained with CM-Dil were injected into the yolk sac of 2 dpf zebrafish, which was the hybrid offspring of miR-144 knockout zebrafish and wild-type zebrafish. Marked zebrafish were observed every 24 hours and photographed by laser scanning confocal microscopy. After 24 hours, osteosarcoma cells started to proliferate and obvious metastasis was observed. After 48 hours, the miR-144 knockout zebrafish showed significant tumor cell proliferation and metastasis compared with wild-type zebrafish. Metastasis to heart, liver and other organs was obviously observed, and noticeable tumor cell masses were enriched in blood islands in miR-144 knockout zebrafish (Figure 5D-F), while wild-type zebrafish showed no apparent tumor metastasis (Figure 5A-C). Thus, these findings revealed that miR-144 inhibited tumorigenesis and metastasis *in vivo*.

Clinical relevance of miR-144 and ROCK1 in osteosarcoma patients

We next aimed to assess whether the relationship of miR-144 and RhoA/ROCK1 could be recapitulated in human osteosarcoma. Patients who were histologically confirmed as having osteosarcoma were enrolled at Shanghai Ninth People's Hospital. Table 1 summarized the relation between the expression of miR-144 and the characteristics of the OS patients. Most tumors displayed osteoblastic histology (82.4 %). The level of miR-144 is significantly down-regulated in the patients developed metastasis during follow-up. Since increased ROCK1 expression was reported to contribute to osteosarcoma progression[Wang, 2013 #28], we examined miR-144, RhoA and

Molecular Pharmacology Fast Forward. Published on January 23, 2019 as DOI: 10.1124/mol.118.114207
This article has not been copyedited and formatted. The final version may differ from this version.

ROCK1 expression in OS tissue samples and normal human bone fragments by immunohistochemistry. Results showed that osteosarcoma specimens had a decreased miR-144 level (Figure 6A) and elevated level of RhoA/ROCK1 expression (Figure 6B) relative to normal osteoblasts. An inverse correlation (R=-0.758) between RhoA/ROCK1 and miR-144 found in osteosarcoma specimens (Figure 6C) further suggests that miR-144 might involves in the progression of RhoA/ROCK1. Furthermore, there was much lower miR-144 expression in three human osteosarcoma cell lines SAOS2, MG63 and U2-OS compared with that in human osteoblastic cell line hFOB1.19 (Figure 6D), while RhoA/ROCK1 mRNA and protein levels were elevated in all three osteosarcoma cell lines (Figure 6D and 6E). Taken together, these data thus suggest that the anti-oncogenic function of miR-144 may largely dependent on the dual-suppressive regulation of RhoA and ROCK1 expression in the malignant progression of osteosarcoma.

Molecular Pharmacology Fast Forward. Published on January 23, 2019 as DOI: 10.1124/mol.118.114207
This article has not been copyedited and formatted. The final version may differ from this version.

Discussion

Previous studies have shown that ROCK1 is frequently overexpressed in multiple categories of cancer, particularly in metastatic tumors. Increased expression of RhoA and ROCK1 is a prognostic indicator associated with metastasis and poor survival in esophageal,[Wang, 2010 #29] breast,[Patel, 2012 #30] and bladder[Kamai, 2003 #31] cancers. During tumor invasion and metastasis, cell migration mediated by actin-myosin contraction is one of the key steps. Rho GTPases are critical regulators of the actin cytoskeleton and cell migration. RhoA is one of the major Rho GTPases involved in these processes. ROCK1 is activated when its C-terminal region binds to RhoA, thus induces the formation of stress fiber[Amano, 1997 #32] and focal adhesion[Ishizaki, 1997 #33] by the phosphorylation of MLC at serine 19 (Ser19). Besides, ROCK1 phosphorylates and activates LIMK, which in turn phosphorylates and inactivates the actin depolymerization factor cofilin. SiRNA-mediated knockdown of ROCK1 caused reorganization of cytoskeleton and decreased cell mobility[Liu, 2009 #34]. Overexpression of a dominant-negative ROCK1 construct or the ROCK-specific inhibitor Y-27632 reduce tumor cell invasion.[Takamura, 2001 #35] In the current study, we observed that ROCK1 expression was relatively higher in osteosarcoma specimens compared with human normal bone, which was consistent with previous reports. Importantly, we found that the expression of ROCK1 and RhoA were regulated by miR-144 in osteosarcoma cell lines.

Accompanied by the upregulation of ROCK1, miR-144 expression is decreased in osteosarcoma specimens and cell lines. miR-144 and miR-451 are transcribed from the same gene locus on human chromosome 17. However, because of the sequence-specific posttranscriptional modulation, the expression levels of miR-144 and miR-451 are different in cells[Rasmussen, 2010 #36]. Downregulation of miR-144 is reported in various cancers[Wang, 2011 #37], suggesting that decreased miR-144 levels are not tumor-type specific and thereby miR-144 may play an important role in tumorigenesis and tumor progression. Ji Woong Son *et al.* performed miRNA microarray and found that miR-144 was down-regulated in non-small cell lung cancer [Ji Woong Son, 2009

#38]. Decreased expression of miR-144 was also found to be correlated with progression of colorectal cancer [Iwaya, 2012 #39]. More recently, Heidi and colleagues reported that miR-144 was found to be downregulated in osteosarcoma [Namlos, 2012 #40]. However, the exact function of miR-144 in cancer has not yet been well elucidated. The tumor suppressive role of miR-144 by targeting ROCK1 in osteosarcoma has been previously reported [Cai, 2015 #42;Wang, 2015 #43]. However, none was reported the rescue effect of ROCK1. It seems that only ROCK1 rescue is not work. In this study, we identified a miR-144 binding site in both ROCK1 and RhoA 3'-UTR by *in silico* analysis and demonstrated that ROCK1 and RhoA are direct targets of miR-144, and overexpression of miR-144 could repress ROCK1 and RhoA protein expression by posttranscriptional regulation. In addition, miR-144 led to a reduction of cell proliferation by blocking cell cycle at G0/G1 phases, and significantly inhibited cell migration and invasion. The tumor-suppressive role of miR-144 was also confirmed in mouse and zebrafish models.

The therapeutic use of miRNAs depends on systemic and/or local application of a specific miRNA-inducing reagent *in vivo*. We complexed synthetic miR-144 with a commercially available *in vivo* jet-polythylenimine (PEI), which had been proved efficient in delivery of miRNAs *in vivo* [Xu, 2011 #41]. During our investigations, the *in vivo* administration of miR-144 for 4 weeks greatly repressed tumor growth in osteosarcoma xenograft mouse model. Immunohistochemical analysis showed that the ROCK1 expression level of osteosarcoma in miR-144-treated mice is much lower than that in the control mice, indicating miR-144 could mediate ROCK1 expression *in vivo*. Also, miR-144 prolonged the overall survival time of tumor-bearing mice, which may result from the anti-proliferative effect of miR-144 on tumor cells. More importantly, miR-144 led to substantial reduction of the dimension and the number of lung nodules in our xenograft model. As this mouse model recapitulates many features of human OS, we may speculate that the suppressive effects of miR-144 on tumor growth and lung metastasis may be beneficial for OS patients.

Molecular Pharmacology Fast Forward. Published on January 23, 2019 as DOI: 10.1124/mol.118.114207
This article has not been copyedited and formatted. The final version may differ from this version.

In conclusion, our findings demonstrated that miR-144 plays a crucial role as a negative upstream regulator of RhoA and its downstream effector ROCK1 through directly targeting their 3'-UTR, inhibiting osteosarcoma tumor cell proliferation, migration and invasion (Figure 7). During osteosarcoma progression, the attenuation of miR-144 expression may be one of the major causes of the upregulation of ROCK1, which ultimately stimulates tumor growth and metastasis. miR-144 functions as a tumor suppressor for osteosarcoma, and the administration of miR-144 appears to be a potentially promising therapeutic strategy for treatment of osteosarcoma.

Molecular Pharmacology Fast Forward. Published on January 23, 2019 as DOI: 10.1124/mol.118.114207
This article has not been copyedited and formatted. The final version may differ from this version.

Authorship Contributions

Participated in research design: Jin Long Liu, Xiao Ling Zhang

Conducted experiments: Jin Long Liu, Jing Li, Jia Jia Xu

Performed data analysis: Jin Long Liu, Fei Xiao, Peng Lei Cui, Zhi Guang Qiao

Wrote or contributed to the writing of the manuscript: Jin Long Liu, Xiao Ling Zhang

References:

Alvarez-Garcia I, Miska EA (2005) MicroRNA functions in animal development and human disease. *Development* **132:** 4653-4662

Amano M, Chihara K, Kimura K, Fukata Y, Nakamura N, Matsuura Y, Kaibuchi K (1997) Formation of actin stress fibers and focal adhesions enhanced by Rho-kinase. *Science* **275:** 1308-1311

Bartel DP (2004) MicroRNAs: genomics, biogenesis, mechanism, and function. *Cell* **116:** 281-297

Betel D, Wilson M, Gabow A, Marks DS, Sander C (2008) The microRNA.org resource: targets and expression. *Nucleic acids research* **36:** D149-153

Bielack SS, Carrle D, Hardes J, Schuck A, Paulussen M (2008) Bone tumors in adolescents and young adults. *Current treatment options in oncology* **9:** 67-80

Cai SD, Chen JS, Xi ZW, Zhang LJ, Niu ML, Gao ZY (2015) MicroRNA144 inhibits migration and proliferation in rectal cancer by downregulating ROCK1. *Molecular medicine reports* **12:** 7396-7402

Cimino D, De Pitta C, Orso F, Zampini M, Casara S, Penna E, Quaglino E, Forni M, Damasco C, Pinatel E, Ponzone R, Romualdi C, Brisken C, De Bortoli M, Biglia N, Provero P, Lanfranchi G, Taverna D (2013) miR148b is a major coordinator of breast cancer progression in a relapse-associated microRNA signature by targeting ITGA5, ROCK1, PIK3CA, NRAS, and CSF1. *FASEB J* **27:** 1223-1235

Croce CM (2009) Causes and consequences of microRNA dysregulation in cancer. *Nature reviews Genetics* **10:** 704-714

Divakaran V, Mann DL (2008) The emerging role of microRNAs in cardiac remodeling and heart failure. *Circulation research* **103:** 1072-1083

Hahmann C, Schroeter T (2010) Rho-kinase inhibitors as therapeutics: from pan inhibition to isoform selectivity. *Cell Mol Life Sci* **67:** 171-177

Harting MT, Blakely ML (2006) Management of osteosarcoma pulmonary metastases. *Seminars in pediatric surgery* **15:** 25-29

Hurst DR, Edmonds MD, Welch DR (2009) Metastamir: the field of metastasis-regulatory microRNA is spreading. *Cancer Res* **69:** 7495-7498

Ishizaki T, Naito M, Fujisawa K, Maekawa M, Watanabe N, Saito Y, Narumiya S (1997) p160ROCK, a Rho-associated coiled-coil forming protein kinase, works downstream of Rho and induces focal adhesions. *FEBS Lett* **404:** 118-124

Iwaya T, Yokobori T, Nishida N, Kogo R, Sudo T, Tanaka F, Shibata K, Sawada G, Takahashi Y, Ishibashi M, Wakabayashi G, Mori M, Mimori K (2012) Downregulation of miR-144 is associated with colorectal

cancer progression via activation of mTOR signaling pathway. *Carcinogenesis* **33:** 2391-2397

Ji Woong Son YJK, Hyun Min Cho, Soo Young Lee, Jin Sung Jang, Jin Eun Choi, Jung Uee Lee, Min Gyu Kang, Yu Mi Lee, Sun Jung Kwon, Eugene Choi, Moon Jun Na, and Jae Yong Park (2009) MicroRNA Expression Profiles in Korean Non-Small Cell Lung Cancer. *Tuberculosis and Respiratory Diseases* **67:** 413-421

Jianwei Z, Fan L, Xiancheng L, Enzhong B, Shuai L, Can L (2013) MicroRNA 181a improves proliferation and invasion, suppresses apoptosis of osteosarcoma cell. *Tumour biology : the journal of the International Society for Oncodevelopmental Biology and Medicine*

Kamai T, Tsujii T, Arai K, Takagi K, Asami H, Ito Y, Oshima H (2003) Significant association of Rho/ROCK pathway with invasion and metastasis of bladder cancer. *Clin Cancer Res* **9:** 2632-2641

Leung T, Chen XQ, Manser E, Lim L (1996) The p160 RhoA-binding kinase ROK alpha is a member of a kinase family and is involved in the reorganization of the cytoskeleton. *Mol Cell Biol* **16:** 5313-5327

Lewis BP, Burge CB, Bartel DP (2005) Conserved seed pairing, often flanked by adenosines, indicates that thousands of human genes are microRNA targets. *Cell* **120:** 15-20

Lin SL, Chiang A, Chang D, Ying SY (2008) Loss of mir-146a function in hormone-refractory prostate cancer. *RNA* **14:** 417-424

Link MP, Goorin AM, Miser AW, Green AA, Pratt CB, Belasco JB, Pritchard J, Malpas JS, Baker AR, Kirkpatrick JA, et al. (1986) The effect of adjuvant chemotherapy on relapse-free survival in patients with osteosarcoma of the extremity. *N Engl J Med* **314:** 1600-1606

Liu S, Goldstein RH, Scepansky EM, Rosenblatt M (2009) Inhibition of rho-associated kinase signaling prevents breast cancer metastasis to human bone. *Cancer Res* **69:** 8742-8751

Liu X, Choy E, Hornicek FJ, Yang S, Yang C, Harmon D, Mankin H, Duan Z (2011) ROCK1 as a potential therapeutic target in osteosarcoma. *J Orthop Res* **29:** 1259-1266

Lu J, Getz G, Miska EA, Alvarez-Saavedra E, Lamb J, Peck D, Sweet-Cordero A, Ebert BL, Mak RH, Ferrando AA, Downing JR, Jacks T, Horvitz HR, Golub TR (2005) MicroRNA expression profiles classify human cancers. *Nature* **435:** 834-838

Maekawa M, Ishizaki T, Boku S, Watanabe N, Fujita A, Iwamatsu A, Obinata T, Ohashi K, Mizuno K, Narumiya S (1999) Signaling from Rho to the actin cytoskeleton through protein kinases ROCK and LIM-kinase. *Science* **285:** 895-898

Mirabello L, Troisi RJ, Savage SA (2009) Osteosarcoma incidence and survival rates from 1973 to 2004: data from the Surveillance, Epidemiology, and End Results Program. *Cancer* **115:** 1531-1543

Nakagawa O, Fujisawa K, Ishizaki T, Saito Y, Nakao K, Narumiya S (1996) ROCK-I and ROCK-II, two isoforms of Rho-associated coiled-coil forming protein serine/threonine kinase in mice. *FEBS Lett* **392:** 189-193

Namlos HM, Meza-Zepeda LA, Baroy T, Ostensen IH, Kresse SH, Kuijjer ML, Serra M, Burger H, Cleton-Jansen AM, Myklebost O (2012) Modulation of the osteosarcoma expression phenotype by microRNAs. *PLoS One* **7:** e48086

Ohashi K, Nagata K, Maekawa M, Ishizaki T, Narumiya S, Mizuno K (2000) Rho-associated kinase ROCK activates LIM-kinase 1 by phosphorylation at threonine 508 within the activation loop. *J Biol Chem* **275:** 3577-3582

Patel RA, Forinash KD, Pireddu R, Sun Y, Sun N, Martin MP, Schonbrunn E, Lawrence NJ, Sebti SM (2012) RKI-1447 is a potent inhibitor of the Rho-associated ROCK kinases with anti-invasive and antitumor activities in breast cancer. *Cancer Res* **72:** 5025-5034

Rasmussen KD, Simmini S, Abreu-Goodger C, Bartonicek N, Di Giacomo M, Bilbao-Cortes D, Horos R, Von Lindern M, Enright AJ, O'Carroll D (2010) The miR-144/451 locus is required for erythroid homeostasis. *J Exp Med* **207:** 1351-1358

Takamura M, Sakamoto M, Genda T, Ichida T, Asakura H, Hirohashi S (2001) Inhibition of intrahepatic metastasis of human hepatocellular carcinoma by Rho-associated protein kinase inhibitor Y-27632. *Hepatology* **33:** 577-581

Tili E, Michaille JJ, Costinean S, Croce CM (2008) MicroRNAs, the immune system and rheumatic disease. *Nature clinical practice Rheumatology* **4:** 534-541

Tu B, Du L, Fan QM, Tang Z, Tang TT (2012) STAT3 activation by IL-6 from mesenchymal stem cells promotes the proliferation and metastasis of osteosarcoma. *Cancer Lett* **325:** 80-88

Wang L, Xue L, Yan H, Li J, Lu Y (2010) Effects of ROCK inhibitor, Y-27632, on adhesion and mobility in esophageal squamous cell cancer cells. *Molecular biology reports* **37:** 1971-1977

Wang W, Peng B, Wang D, Ma X, Jiang D, Zhao J, Yu L (2011) Human tumor microRNA signatures derived from large-scale oligonucleotide microarray datasets. *International journal of cancer Journal international du cancer* **129:** 1624-1634

Wang W, Zhou X, Wei M (2015) MicroRNA-144 suppresses osteosarcoma growth and metastasis by targeting ROCK1 and ROCK2. *Oncotarget* **6:** 10297-10308

Wang Y, Zhao W, Fu Q (2013) miR-335 suppresses migration and invasion by targeting ROCK1 in osteosarcoma cells. *Molecular and cellular biochemistry*

Xu D, Takeshita F, Hino Y, Fukunaga S, Kudo Y, Tamaki A, Matsunaga J, Takahashi RU, Takata T,

Molecular Pharmacology Fast Forward. Published on January 23, 2019 as DOI: 10.1124/mol.118.114207
This article has not been copyedited and formatted. The final version may differ from this version.

Shimamoto A, Ochiya T, Tahara H (2011) miR-22 represses cancer progression by inducing cellular senescence. *J Cell Biol* **193:** 409-424

Zheng B, Liang L, Wang C, Huang S, Cao X, Zha R, Liu L, Jia D, Tian Q, Wu J, Ye Y, Wang Q, Long Z, Zhou Y, Du C, He X, Shi Y (2011) MicroRNA-148a suppresses tumor cell invasion and metastasis by downregulating ROCK1 in gastric cancer. *Clin Cancer Res* **17:** 7574-7583

Molecular Pharmacology Fast Forward. Published on January 23, 2019 as DOI: 10.1124/mol.118.114207
This article has not been copyedited and formatted. The final version may differ from this version.

Footnotes

This work was supported by grants from The Ministry of Science and Technology of China (No.2011DFA30790), National Natural Science Foundation of China (No. 81190133, No.31101056), Chinese Academy of Sciences (No.XDA01030404, KSCX2-EW-Q-1-07), Science and Technology Commission of Shanghai Municipality (No. 12411951100, 12410708600), Shanghai Municipal Education Commission (No.J50206), Shanghai Jiao Tong University (No. 2202012114), and National Institute of Health (RO1AG017021).

Molecular Pharmacology Fast Forward. Published on January 23, 2019 as DOI: 10.1124/mol.118.114207
This article has not been copyedited and formatted. The final version may differ from this version.

Figure legends

Figure 1. miR-144 functions as a tumor suppressor in osteosarcoma cells. (A) In vitro growth of control and miR-144 mimic transfected SAOS2 and U2-OS cells are measured by Alamar Blue assay (n=3). (B) Cell cycle distribution of control and miR-144 mimic transfected SAOS2 and U2-OS cells are evaluated by FACS analysis. The representative flow cytometry pattern is shown in left panel. Relative percentages of the cell population in different phases were presented in the total gated cell numbers shown in right panel (n=3). (C) In vitro soft agar assays examining the anchorage-independent growth of control and miR-144 mimic transfected SAOS2 and U2-OS cells, and quantitation results are shown in right panel (n=3). (D-E) In vitro transwell (D) and wound-healing assay (E) examining the migration and invasion abilities of control and miR-144 mimic transfected SAOS2 and U2-0S cells, and quantitation results are shown in right panel (n=3). The data are presented as the mean ± S.D. (n = 3). Significant differences were analyzed using Student's t test compared with miR-NC group and marked with asterisks (*$P < 0.05$, ** $P < 0.01$).

Figure 2. ROCK1 and RhoA are direct targets of miR-144. (A) WB analysis of ROCK1 and RhoA in control and miR-144 mimic transfected SAOS2 and U2-OS cells, quantitation results are shown in right panel. (B) Pulldown assay revealed a more enrichment of ROCK1 and RhoA 3'UTR in the miR-144-captured fraction compared with the introduction of miR-144 mutation that disrupted the binding site of miR-144 for ROCK1/RhoA 3'UTR. (C) Up: WB analysis of anti-AGO2 RNA immunoprecipitation from HEK293T. Down: Relative miR-144, ROCK1 and RhoA mRNA expression from anti-AGO2 RNA immunoprecipitation. (D) Sequence of the miR-144 binding sites within ROCK1 and RhoA 3'-UTR (upper left) and a schematic diagram of the reporter constructs showing the ROCK1 and RhoA 3'-UTR sequence (ROCK1-WT; RhoA-WT) and the mutated ROCK1 and RhoA 3'-UTR sequence (ROCK1-Mut; RhoA-Mut, the mutant nucleotides of the miR-144 binding sites are in red, lower left). Luciferase activity of the ROCK1-WT and ROCK1-Mut reporter (upper right) and RhoA-WT and RhoA-Mut reporter (lower right) with miR-144 mimic

or control. The data are presented as the mean ± S.D. (n = 3). Significant differences were analyzed using Student's t test for A and Dunnett's or Tukey-Kramer's tests, as post-hoc tests following the analysis of variance (ANOVA) for B-D, marked with asterisks (*$P < 0.05$, ** $P < 0.01$).

Figure 3. miR-144 regulates ROCK1 and RhoA to inhibit osteosarcoma tumorigenesis. (A) WB analysis of ROCK1 and RhoA in miR-144 mimic transfected SAOS2 and U2-OS cells with control and ROCK1, RhoA or both transfection, and quantification results are shown in right panel. (B) Left: In vitro growth of miR-144 mimic transfected SAOS2 and U2-OS cells with control and ROCK1, RhoA or both transfection (n=3). (C) FACS analyses showing cell cycle distribution of miR-144 mimic transfected SAOS2 and U2-OS cells with control and ROCK1, RhoA or both transfection (n=3). (D-E) In vitro transwell (D) and wound-healing assay (E) examining the migration and invasion abilities of miR-144 mimic transfected SAOS2 and U2-OS cells with control and ROCK1, RhoA or both transfection. The data are presented as the mean ± S.D. (n = 3). Significant differences were analyzed using Dunnett's or Tukey-Kramer's tests, as post-hoc tests following the analysis of variance (ANOVA) for B-D, marked with asterisks (*$P < 0.05$, ** $P < 0.01$).

Figure 4. miR-144 inhibits tumorigenesis and metastasis *in vivo*. (A) The elevated miR-144 level in the xenograft tumors was confirm by qRT-PCR. (B) Left: tumor volume of xenografts in nude mice injected SAOS2 cells with control or miR-144 oligo nucleotides treatment (n=10). Middle: representative images of NC and miR-144-treated tumors. Right: representative in vivo imaging photos of NC and miR-144-treated NOD mice. (C) Animal survival of tumorigenesis analysis of SAOS2 cells with NC and miR-144 treatment in nude mice. (D) H&E, miRNA-144 ISH and RCOK1/RhoA IHC stained images of tibia sections from NC and miR-144-treated mice. The data are presented as the mean ± S.D. (n = 3). Significant differences in B were analyzed using Dunnett's or Tukey-Kramer's tests, as post-hoc tests following the

Molecular Pharmacology Fast Forward. Published on January 23, 2019 as DOI: 10.1124/mol.118.114207
This article has not been copyedited and formatted. The final version may differ from this version.

analysis of variance (ANOVA) for B-D, marked with asterisks (** $P < 0.01$). The Kaplan-Meier analysis in C was used to estimate the overall survival, and the log-rank test was used to evaluate the differences between survival curves.

Figure 5. miR-144 inhibits tumor metastasis *in vivo*. Images of WT and miR-144 knockout (KO) zebrafish injected with CM-Dil stained SAOS2 cells showing the tumorigenic progression and metastasis to heart and blood islands at 2 dpi (n=3).

Figure 6. Clinical relevance of miR-144 and RhoA/ ROCK1 in osteosarcoma patients. Real-time PCR analysis of miR-144 (A), RhoA and ROCK1 (B) in normal human bone and osteosarcoma. (C) The co-relation between miR-144 and ROCK1 and RhoA were analysis in normal human bone and osteosarcoma. (D) Real-time PCR analysis of miR-144, ROCK1 and RhoA in human osteoblastic cell line hFOB1.19 and osteosarcoma cell lines SAOS2, MG63 and U2-OS. (E) Western blot analysis of ROCK1 and RhoA in human osteoblastic cell line hFOB1.19 and osteosarcoma cell lines SAOS2, MG63 and U2-OS. Results are presented as mean ± SD. **$P < 0.01$, ***$P < 0.001$. The data are presented as the mean ± S.D. (n = 3). Significant differences were analyzed using Student's t test for A-B and Dunnett's or Tukey-Kramer's tests, as post-hoc tests following the analysis of variance (ANOVA) for D-E (*$P < 0.05$, ** $P < 0.01$, *** $P < 0.001$). The correlation analysis in C was using Pearson chi-square test.

Figure 7. Model of miR-144 in osteosarcoma tumorigenesis. MiR-144 inhibits tumor growth and metastasis in osteosarcoma via dual-targeting RhoA and its downstream effector ROCK1.

Molecular Pharmacology Fast Forward. Published on January 23, 2019 as DOI: 10.1124/mol.118.114207
This article has not been copyedited and formatted. The final version may differ from this version.

Table 1. Association between miR-144-3p expression and characteristics of patients with osteosarcoma. P-values were obtained from Pearson chi-square test or Fisher's exact test.

Variables	No.of cases	Expression of miR-144-3p		P value
		Low	High	
Age				0.504
<21	25	12	13	
≥21	26	11	14	
Gender				
Male	33	18	15	0.639
Female	18	10	8	
Location				0.412
Distal	16	9	7	
Proximal	35	19	16	
Histological type				
Osteoblastic	41	18	23	
Chondroblastic	5	2	3	
Fibroblastic	5	3	2	
TNM Stage				<0.001
I+II	31	10	21	
III+IV	16	11	5	
Distant Metastasis				<0.001
No	22	14	8	
Yes	29	23	6	

Molecular Pharmacology Fast Forward. Published on January 23, 2019 as DOI: 10.1124/mol.118.114207
This article has not been copyedited and formatted. The final version may differ from this version.

Table 2. Primer sequences used for real-time PCR.

	Sense primer (5'-3')	Antisense primer (5'-3')
miR-144	GCGTGCTACAGTATAGATGATG	GTGCAGGGTCCGAGGT
U6	CTCGCTTCGGCAGCACA	AACGCTTCACGAATTTGCGT
ROCK1	AACATGCTGCTGGATAAATCTGG	TGTATCACATCGTACCATGCCT
RhoA	TTTGGAGGTGGCATAGCCTT	ATGTTTAGTCAGCTGGAGAGAAGAG
GAPDH	ACAACTTTGGTATCGTGGAAGG	GCCATCACGCCACAGTTTC

Molecular Pharmacology Fast Forward. Published on January 23, 2019 as DOI: 10.1124/mol.118.114207
This article has not been copyedited and formatted. The final version may differ from this version.

MOL # 114207

Figure 1

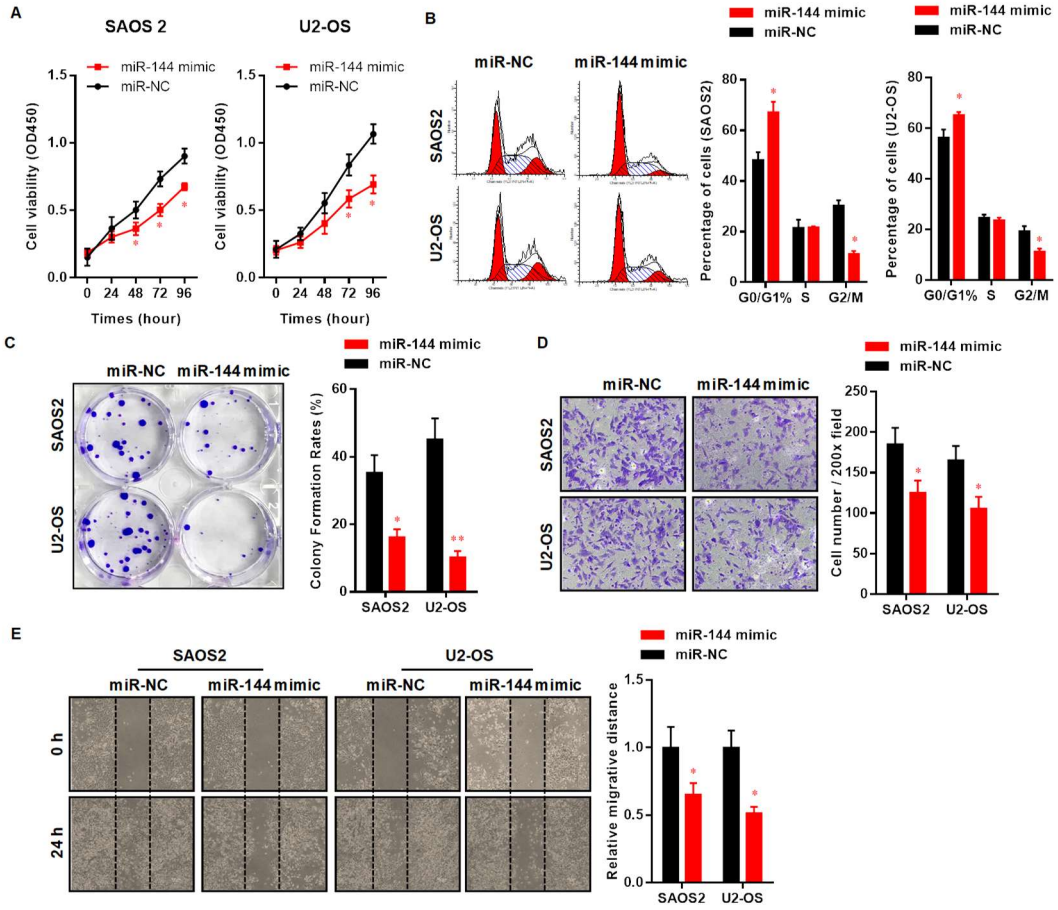

Molecular Pharmacology Fast Forward. Published on January 23, 2019 as DOI: 10.1124/mol.118.114207
This article has not been copyedited and formatted. The final version may differ from this version.

Figure 2

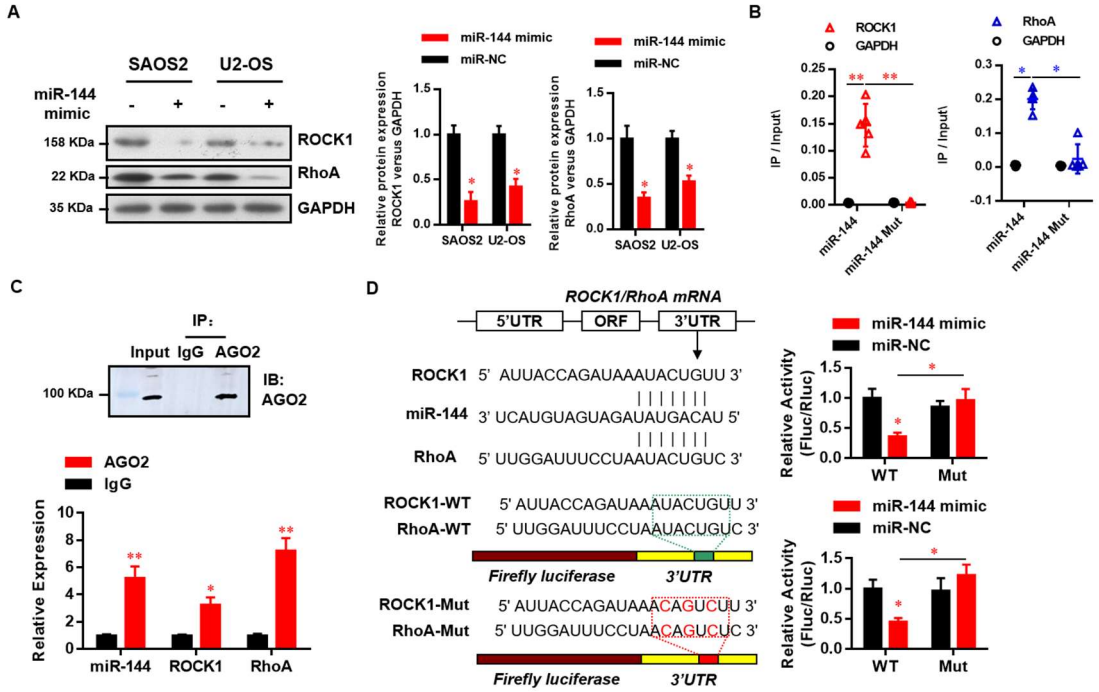

Molecular Pharmacology Fast Forward. Published on January 23, 2019 as DOI: 10.1124/mol.118.114207
This article has not been copyedited and formatted. The final version may differ from this version.

Figure 3

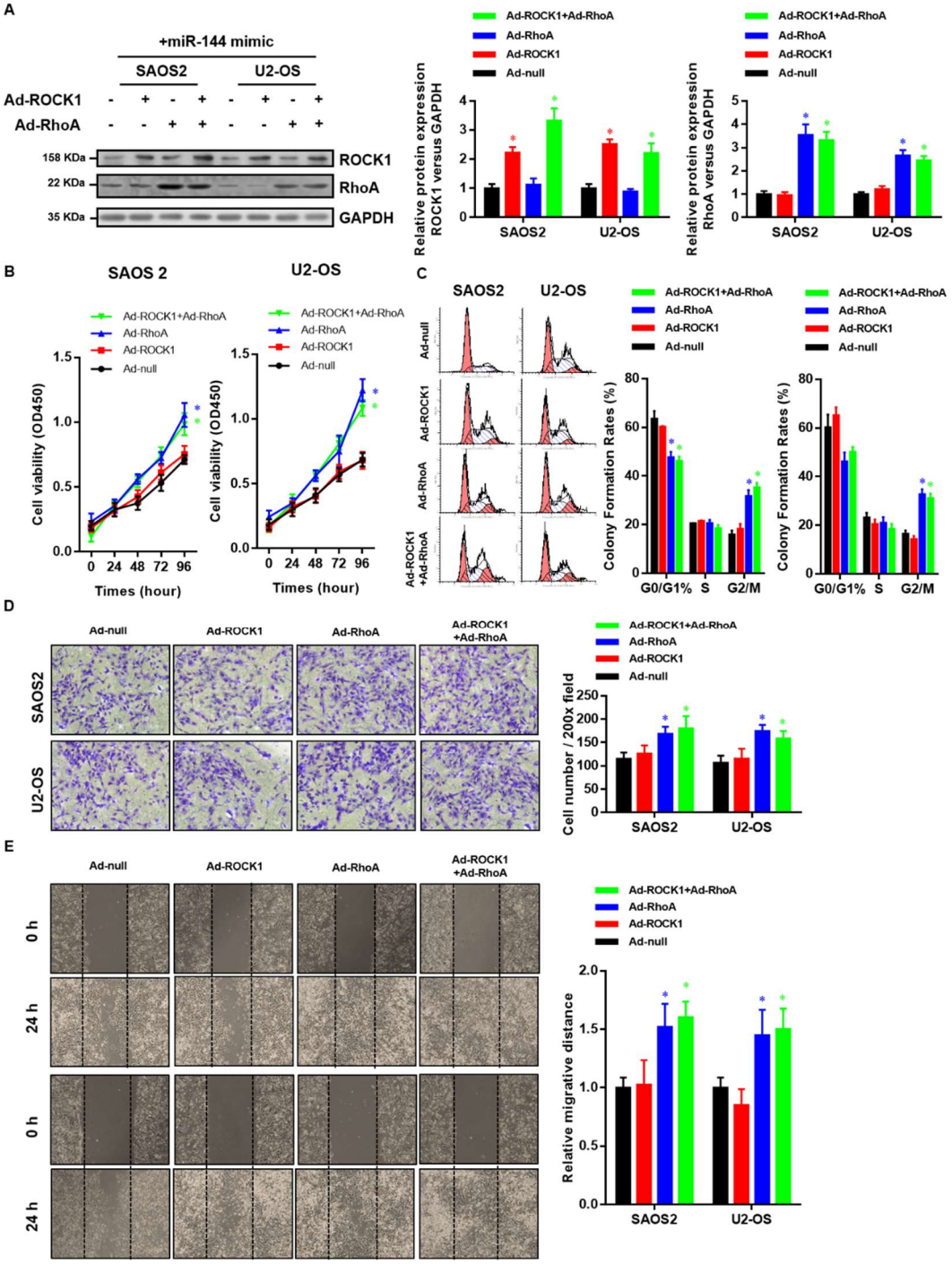

Molecular Pharmacology Fast Forward. Published on January 23, 2019 as DOI: 10.1124/mol.118.114207
This article has not been copyedited and formatted. The final version may differ from this version.

MOL # 114207

Figure 4

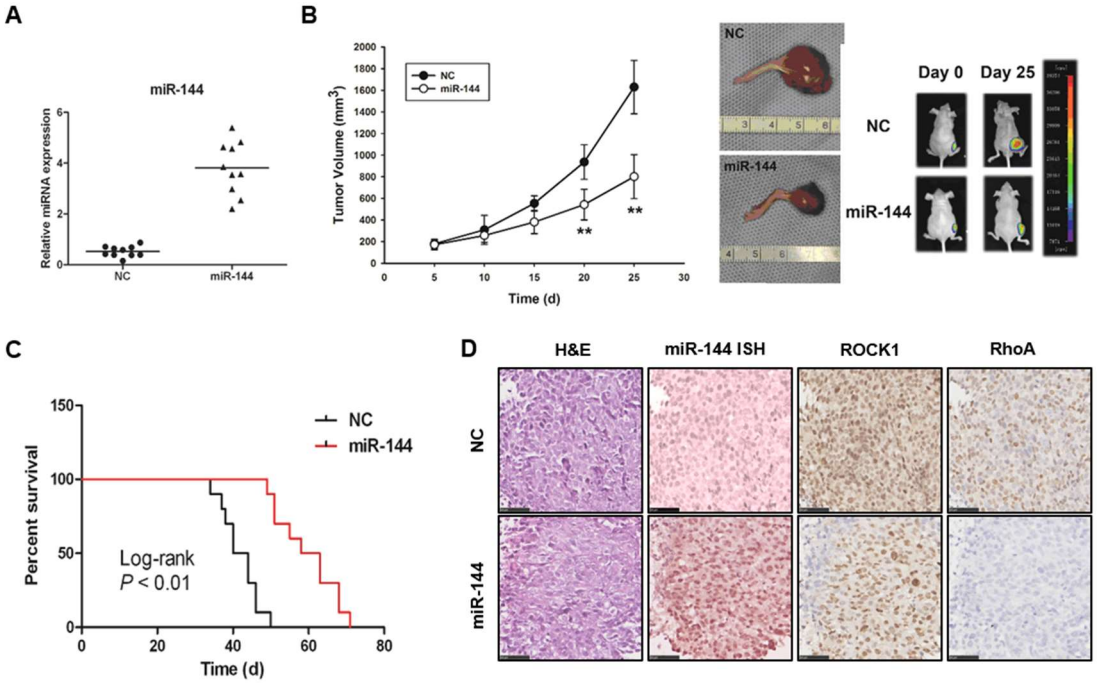

Molecular Pharmacology Fast Forward. Published on January 23, 2019 as DOI: 10.1124/mol.118.114207
This article has not been copyedited and formatted. The final version may differ from this version.

MOL # 114207

Figure 5

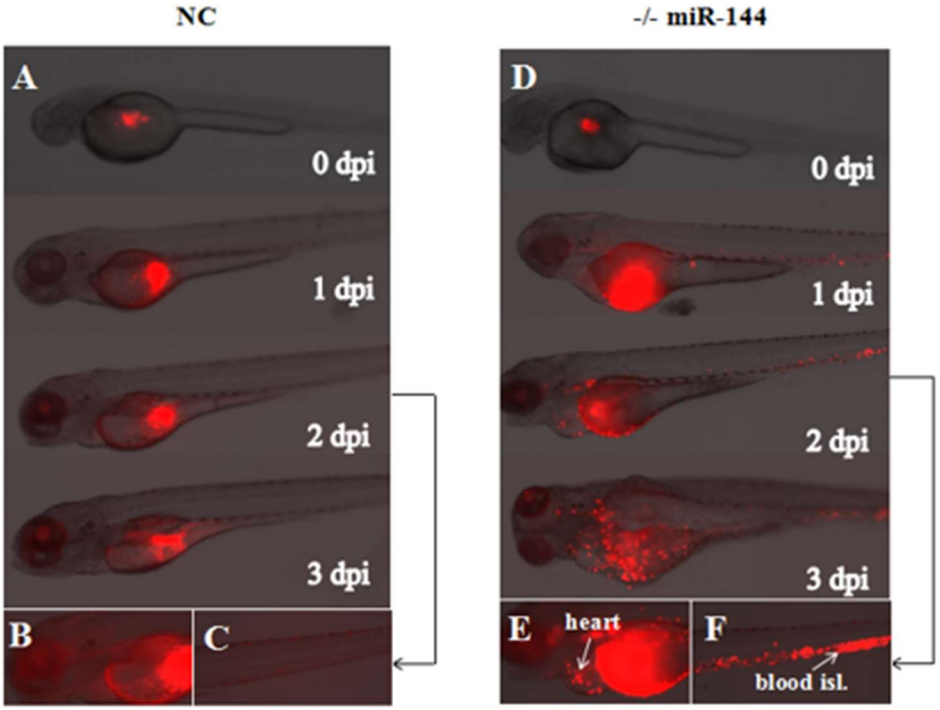

Molecular Pharmacology Fast Forward. Published on January 23, 2019 as DOI: 10.1124/mol.118.114207
This article has not been copyedited and formatted. The final version may differ from this version.

MOL # 114207

Figure 6

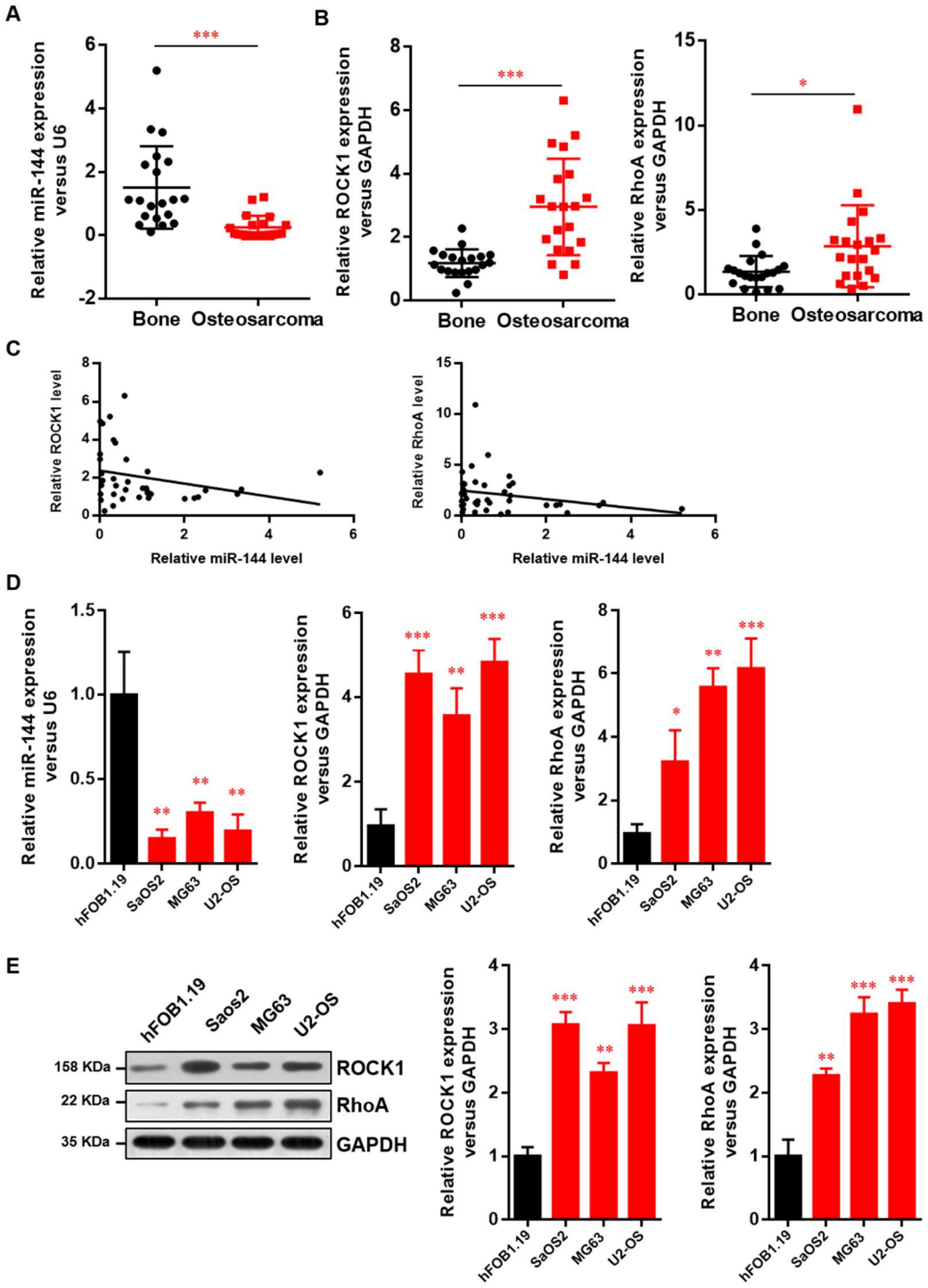

Molecular Pharmacology Fast Forward. Published on January 23, 2019 as DOI: 10.1124/mol.118.114207
This article has not been copyedited and formatted. The final version may differ from this version.

MOL # 114207

Figure 7